Materials Horizons

ROYAL SOCIETY OF CHEMISTRY

COMMUNICATION

View Article Online
View Journal | View Issue

Cite this: *Mater. Horiz.*, 2020, 7, 2959

Received 11th May 2020,
Accepted 20th August 2020

DOI: 10.1039/d0mh00785d

rsc.li/materials-horizons

Acid dyeing for green solvent processing of solvent resistant semiconducting organic thin films†

Cayley R. Harding,[a] Jonathan Cann,[a] Audrey Laventure,[a] Mozhgan Sadeghianlemraski,[b] Marwa Abd-Ellah,[ab] Keerthan R. Rao,[d] Benjamin Sidney Gelfand,[a] Hany Aziz,[b] Loren Kaake,[c] Chad Risko[d] and Gregory C. Welch *[a]

The alcohol and water-based processing of a perylene diimide (PDI) organic semiconductor into large area and solvent resistant films is reported. The compound, PDIN-H, is an N-annulated PDI dye with a pyrrolic NH functional group that can be deprotonated to render the material soluble in polar solvents. Addition of NaOH to mixtures of PDIN-H in 1-propanol results in a progressive color change from orange/red to purple with increasing equivalents of base. Use of 1 molar equivalent of NaOH was found to fully dissolve the PDIN-H in alcohol solvents up to a concentration of 10 mg mL^{-1}. Primary alcohols 1-propanol to 1-hexanol as well as 2-propanol were used. All solutions were readily spin-coated or slot-die coated into uniform thin films. Solutions in 1-propanol could be coated with concentrations up to 50 mg mL^{-1}. All films were red in color and characterized by optical absorption spectroscopy confirming the existence of the parent PDIN-H species in the film. Single crystal X-ray diffraction was used to determine the molecular packing of PDIN-H. Films showed no signs of dewetting, swelling, or dissolution upon exposure to 2-propanol, water, or *o*-xylene *via* coating or dipping indicating they were solvent resistant. To exploit the semiconducting properties of these PDIN-H films, organic photovoltaic devices were fabricated using the films as electron transport layers in inverted type P3HT:PC$_{61}$BM bulk heterojunction devices. Moreover, the PDIN-H films changed from red to purple upon exposure to butylamine vapors which prompted the investigation of hydroxide free processing. Indeed, films of PDIN-H were easily formed by processing with 1-propanol/butylamine or water/butylamine solutions.

New concepts

In the quest towards green electronics, the formation of electronically active films from green solvents that enables multi-layer device fabrication is a key challenge. In this contribution we demonstrate how the classic concept of acid dyeing can be used to deliver a materials system that can be roll-to-roll compatible processed from alcohol or water into solvent resistant semiconducting films. While prior work has mostly focused on polymer-based systems with cleavable side chains to yield films, we have utilized a simple, yet versatile, molecular system based on the popular perylene diimide chromophore. Functionalization with a pyrrolic NH bond has a dual system enhancement. First, the NH group can be polarized to enable alcohol or water processing while second, the NH group participates in hydrogen bonding with an adjacent molecule strengthening intermolecular interactions, thus leading to solvent resistant film. This study lays the groundwork for the development of next-generation green electronics and has uncovered a new materials design concept for which one can envision a myriad of new structures being developed.

Introduction

Perylene diimide (PDI) dyes have a long history as stable colorants with uses as diverse as textile dyes, print media, and automotive paints.[1,2] The extended π-conjugated structure yields strong visible light absorption and deep lying frontier molecular orbital (FMO) energies.[3–5] In addition, the molecules self-assemble into structures with strongly overlapping π-stacks rendering this chromophore appropriate as an electron transport

[a] *Department of Chemistry, University of Calgary, 2500 University Drive N.W., Calgary, Alberta, T2N 1N4, Canada. E-mail: gregory.welch@ucalgary.ca*
[b] *Department of Electrical and Computer Engineering, University of Waterloo, Waterloo, Ontario, N2L 3G1, Canada*
[c] *Department of Chemistry, Simon Fraser University, Vancouver, British Columbia, V5A 1S6, Canada*
[d] *Department of Chemistry & Center for Applied Energy Research, University of Kentucky, Lexington, Kentucky, 40506, USA*

† Electronic supplementary information (ESI) available: Materials and methods. PDIN-H solubility images in various solvents. Deprotonation/protonation reversibility. Films dipped in solvent images. UV-vis of film exposure to amine vapors. PDIN-H films spin cast and slot-die coated from 1-propanol/butylamine and water/butylamine images and UV-vis. Films cast from 1-propanol/butylamine and water/butylamine with solvents slot-die coated on top images and UV-vis. Safety comment and hazards information. CCDC 2003001. For ESI and crystallographic data in CIF or other electronic format see DOI: 10.1039/d0mh00785d

material in optoelectronic devices.[6–8] This organic polycyclic aromatic building block has been used to prepare a myriad of functional materials for use in electronic devices including photovoltaics,[9] light emitting diodes,[10] and field-effect transistors.[11] A key feature of PDI is that its self-assembly properties can be further optimized by modifying the core at the bay, headland, and imide positions. This level of control is critical to tune its morphology in the solid-state for realizing high organic electronic device performance.[12,13]

Of unique importance is controlling both the molecular properties and self-assembly in thin films *via* heteroatom annulation at the bay position of the PDI chromophore. Sulphur,[14,15] selenium,[16,17] and nitrogen[18,19] annulation have all been explored to create new classes of PDIs.[20,21] As we have previously demonstrated,[22–25] N-annulation destabilizes the FMO energies and provides an extra site for side-chain engineering.[26,27] These alterations have led to the development of non-fullerene acceptors (NFAs) for organic photovoltaic (OPV) applications. In particular, OPV devices based on these NFAs exhibit large open circuit voltages >1 V and can be coated using non-halogenated solvents *via* roll-to-roll compatible methods.[28–32]

Processing from benign solvents is a necessity for the commercialization of organic electronic materials. Concern about adverse health and environmental effects of the materials, processing solvents, and devices at end of use is mounting.[33–36] Specifically, halogenated aromatic solvents such as 1,2-dichlorobenzene and chlorobenzene are often used despite their toxicity and low vapour pressure. Such solvents pose safety hazards to human and environment health and as such, large scale industrial production can no longer target methods that require these halogenated and aromatic solvents. Specifically, for OPV technologies, much effort is being dedicated to green solvent processing.[37,38] A selection guide summarizes the ''greenness'' of common solvents *via* safety, health and environmental criteria for further information.[39]

Replacing halogenated solvents is no easy task using currently available materials. Stringent requirements on the solubility, uniformity of film formation, and self-assembly into ideal nanomorphologies[40] have made aromatic and halogenated solvents the most common processing solvents for device fabrication with standard alkylated π-conjugated materials.[37,41] The molecule and solvent can no longer be thought of as independently optimizable parameters, making device fabrication with green solvents both a tremendous challenge and research opportunity.[42,43]

An additional challenge is to not only develop materials that can be processed from green solvents,[44] but to prepare films that can be rendered solvent resistant enabling multi-layer devices.[45] This challenge looms especially large with a more limited solvent palette that is typically employed in so-called ''orthogonal processing'' (*i.e.* forming multilayer organic films using sequentially immiscible solvents). One common method to impart solvent resistance that enables orthogonal processing is to modify a semiconducting polymer with a cleavable or crosslinkable side-chain.[45–47] These approaches have their disadvantages. Solvent resistance imparted by cleavable side-chains is inherently not atom-economical. Solvent resistance imparted by crosslinkable side-chains requires post-deposition treatment such as thermal or UV annealing. A third method developed by the groups of Reynolds and Reichmanis is the use of an ester or acid modified alkyl chain appended to the materials conjugated backbone.[42,43] Upon treatment with hydroxide base, in this case a conjugated polymer, the material becomes water soluble and thus can be cast into a film from this green solvent. In Reynolds' system, UV-treatment results in side-chain cleavage rendering the film solvent resistant, while for Reichmanis' system a mild acid treatment leaves the film impervious to various solvents. For the latter, this is analogous to the process of acid dyeing wherein a dye molecule containing an acidic functional group (typically sulfonic acids) can be deprotonated to increase aqueous solubility. A textile can be immersed in the solution of the anionic dye and exposed to acid to protonate the dye and permanently color the textile. Acid dyeing is a robust method to generate highly resistant coloured fabrics while still retaining high solubility in water.[48] As such we took inspiration from both acid dyeing as well as the work of Reichmanis to develop an acid dye process to produce solvent resistant thin films for organic electronics.

In this report we expand these works into an intrinsically acidic molecular system and demonstrate how the N-annulated PDI can be rendered alcohol or water soluble by deprotonation. Upon drying, the film spontaneously protonates to form a solvent resistant semiconducting film. Critical is the presence of a pyrrolic N–H site which can be deprotonated to yield an ionic molecule soluble in polar solvents and when protonated in the solid-state, participates in hydrogen bonding, contributing to the solvent resistant property of the film.

Results and discussion

The N-annulated PDI (PDIN-H, Fig. 1) can be readily synthesized and purified column chromatology free, on multi-gram scale.[22] The compound is bright red and is only sparingly soluble in halogenated solvents such as $CHCl_3$ or polar solvents such as propanol (Fig. S1, ESI†). Upon addition of NaOH to a slurry of 1-propanol and PDIN-H (10 mg mL^{-1}) a color change from orange/red to purple and complete dissolution of the PDIN-H is observed. Spin-coating this solution onto an anti-static coated polyethylene terephthalate (PET) substrate results in the formation of a uniform red thin-film. In this process the NaOH is deprotonating the PDIN-H creating an alcohol soluble ionic dye, $PDIN^{-}Na^{+}$. *Via* established density functional theory (DFT) protocols,[49–54] here at the M06/6-31G(d,p) level of theory[55–58] with the SMD model[59] and a dielectric medium representing 1-propanol ($\varepsilon = 20.52$), we estimate the pK_a of PDIN-H to be 19.7. A transition from solution to film shifts back to the PDIN-H giving the distinct neutral PDI red color (Fig. 1).

This process was further investigated in dilute solution using optical absorption spectroscopy (Fig. 2). In dilute $CHCl_3$ solution, PDIN-H gives rise to a typical PDI based absorption spectrum with strong absorption from 400–550 nm with three diagnostic vibronic bands. Adding base to this solution has no effect. For solutions of PDIN-H in 1-propanol (PDIN-H concentration of 0.01 mg mL^{-1}), a gradual change in color from orange to purple

Fig. 1 Chemical structure of PDIN-H. Treatment of a 10 mg mL^{-1} slurry of PDIN-H in 1-propanol with 1 molar equivalent of NaOH produces a purple ionic solution. Spin-coating this solution onto a PET substrate yields a red colored organic film owing to the spontaneous protonation of the $PDIN^-$ anion. This processes mimics that of classic acid dyeing of textiles.

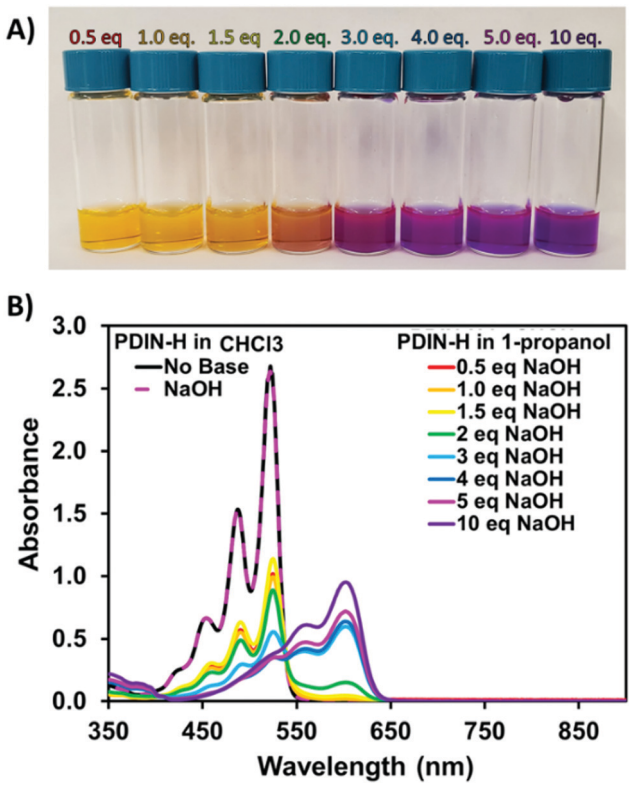

Fig. 2 (A) Image showing the color changes of PDIN-H in 1-propanol solution with varying equivalents of NaOH added. (B) UV-vis spectra of PDIN-H solutions in $CHCl_3$ with 1 mol equivalent NaOH, and in 1-propanol with 0–10 mol equivalents of NaOH.

with increasing equivalents of NaOH added (up to 10 molar equivalents) was observed. The gradual change in dilute solution suggests an equilibrium in favor of the PDIN-H. UV-visible spectroscopic analysis of the solutions reveals that at 0.5 eq. NaOH added, the dominant absorption profile of PDIN-H is present with characteristic PDI bands at 459, 490, and 525 nm. At 1.0 eq. NaOH added a small lower energy band at 601 nm appears. This new band is attributed to the $PDIN^-$ anion.[60] The red-shift (0.64 eV) is expected as the deprotonation adds a lone pair of electrons to the pyrrolic N-atom, increasing electron density, and subsequently destabilizing the HOMO and LUMO energies and narrowing the bandgap. Indeed, DFT and time-dependent DFT (TDDFT) calculations, both at the M06/6-31G(d,p) level theory (in the gas phase), confirm this hypothesis. The HOMO and LUMO (Fig. 3) for both PDIN-H and $PDIN^-$ share similar spatial distributions, as one may expect. Deprotonation of PDIN-H to form the $PDIN^-$ anion, however, results in a considerable energetic destabilization of both the HOMO (from −6.17 eV in PDIN-H to −2.87 eV in $PDIN^-$) and LUMO (from −3.11 eV in PDIN-H to +0.33 eV in $PDIN^-$). Notably, the HOMO–LUMO gap of $PDIN^-$ is 0.19 eV smaller than that of PDIN-H. This smaller HOMO–LUMO gap for $PDIN^-$ correlates well with the red-shifted $S_0 \rightarrow S_1$ vertical transition for $PDIN^-$ (534 nm, 2.32 eV) compared to PDIN-H (476 nm, 2.61 eV), as both $S_0 \rightarrow S_1$ transitions are described predominantly by a one-electron excitation from HOMO → LUMO (95% electronic configuration for $PDIN^-$, and 98% electronic configuration for PDIN-H). These one-electron transitions, and simulated absorption spectra derived through convolution of the vertical transition energies and oscillator strengths with Gaussian functions, correlate well with data derived from UV-vis spectroscopy. At 2.0 eq. NaOH the two species have near equal absorbance intensity. At 10.0 eq. NaOH it appears that the PDIN-H is fully deprotonated giving rise to an absorbance spectrum of only the $PDIN^-$ anion, characteristics which have been observed in other PDI based molecules.[61,62] The high concentration of NaOH implies an equilibrium exists for this system. The process is fully reversible upon addition of protic acid (Fig. S2, ESI†).

To expand the solvent scope for solution preparation and subsequent film formation a series of five alcohols were tested and solutions both spin-coated (spin-cast) and slot-die coated onto PET substrates. Alcohols were the solvent of choice, as they have an appropriate drying rate for large scale printing techniques, and were chosen over other green solvents such as esters or hydrocarbons as they tend to show better EHS (environmental, health and safety) properties,[63] as well they

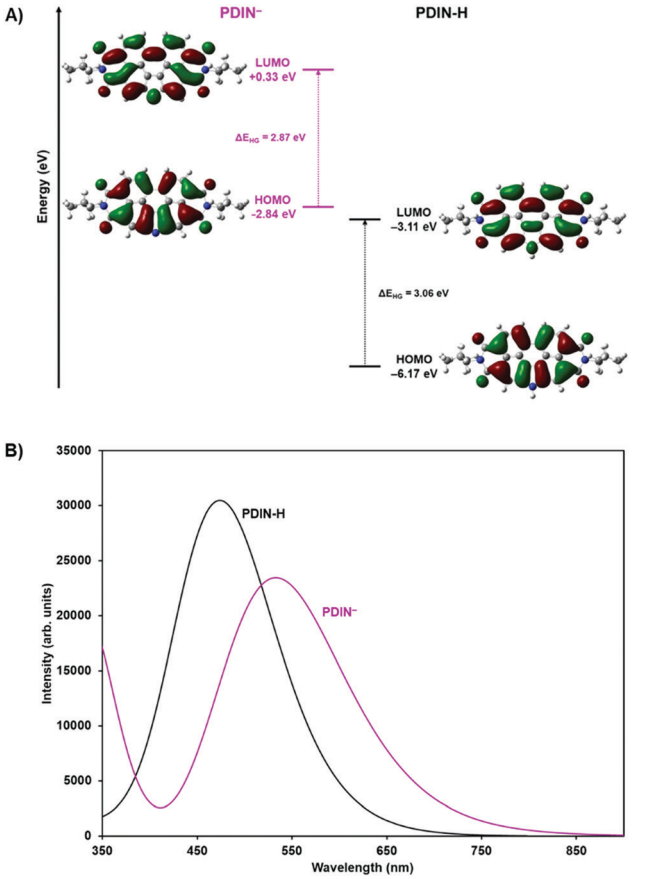

Fig. 3 (A) Schematic molecular orbital (MO) correlation diagram for $PDIN^-$ (left, purple) and PDIN-H (right, black) as determined at the M06/6-31G(d,p) level of theory. (B) Simulated absorption spectra of $PDIN^-$ (purple) and PDIN-H (black) derived from TDDFT calculations at the M06/6-31G(d,p) level of theory.

Fig. 4 (A) Top – images of spin-coated (SC) 1.5 cm × 1.5 cm films. Bottom – images of slot-die coated (SD) 13 mm × 20 cm films, (1) 2-propanol, (2) 1-propanol, (3) 1-butanol, (4) 1-pentanol, (5) 1-hexanol. Films prepared from 10 mg mL^{-1} solutions of PDIN-H in alcohol with 1 molar equivalent of NaOH added. (B) Images of slot-die coated films from 1-propanol solutions with varying PDIN-H concentrations. (6) 5 mg mL^{-1}, (7) 10 mg mL^{-1}, (8) 20 mg mL^{-1}, (9) 30 mg mL^{-1}, (10) 40 mg mL^{-1}, (11) 50 mg mL^{-1}. For all solutions 1 molar equivalent of NaOH was added.

solubilize the sodium hydroxide necessary for our system to work. Multiple PDIN-H/NaOH solutions were prepared at 10 mg mL^{-1} in the following alcohols: 2-propanol, 1-propanol, 1-butanol, 1-pentanol, and 1-hexanol. Only 1 molar equivalent of NaOH was required to solubilize the PDIN-H. Methanol failed to yield solutions suitable for uniform film formation as the PDIN-H did not dissolve and thus could not be converted to the anion. The longer chain alcohols 1-heptanol and 1-decanol were not suitable for roll-to-roll coating methods owing to low vapour pressures and correspondingly long drying times (>12 hours at room temperature). 1-Octanol and 1-nonanol were not tried as they are environmental hazards (see ESI,† Appendix S1). Evaluating solutions for scalable film deposition methods rather than spin-coating is important in demonstrating a material's relevance for large scale manufacturing. Slot-die coating has been identified as a viable method for the roll-to-roll coating of organic semiconducting films with several reports detailing the practical use of the technique.[64–68] We faced no challenges in either spin-coating or slot-die coating the solutions and, in all cases, uniform films were formed with no visible defects or particles (Fig. 4A). The purple solutions remained purple upon initial coating of the PET substrate, but as solvent evaporation occurred the resulting films were red in color.

Controlling film thickness is important in a variety of contexts, making it necessary to deposit films from a wide range of solution concentrations. Solutions of PDIN-H/NaOH were prepared with PDIN-H concentrations of 5, 10, 20, 30, 40, and 50 mg mL^{-1} with 1 molar equivalent of NaOH added. Inks were purple in color with no visible solids. Upon slot-die coating, the inks yielded highly uniform thin films (Fig. 4B).

Optical absorption spectroscopy can be used to understand the molecular packing within the thin-film and determine relative film thickness based on light absorption, thus all films were analyzed using UV-visible spectroscopy (Fig. 5). All films exhibited the same basic optical absorption profile with a dominant absorption band from 380 nm to 625 nm with λ_{max} at 498 nm and a low energy shoulder at 524 nm. This profile has been seen previously in thin films of PDI monomers.[69,70] For the spin-coated films an increase in light absorption is observed with an increase in the vapour pressure of the alcohol (Fig. 5A). This is consistent with the notation that higher vapor pressure solvents evaporate quicker during spin-coating and leave more material on the substrate. For the slot-die coated films from different alcohols, the optical absorption profiles remain constant, consistent with all material being deposited on the substrate (Fig. 5B). Not surprisingly, increasing the concentration from 5 to 50 mg mL^{-1} results in a progressive increase in light absorption (Fig. 5C). The optical absorption profile of an organic conjugated material in the film is known to be sensitive to morphology and aggregation.[71,72] Considering the optical profiles are more similar than different we do not expect major differences in the molecular packing.

As mentioned, multi-layer device formation requires that the deposited films can be made solvent resistant in respect to the

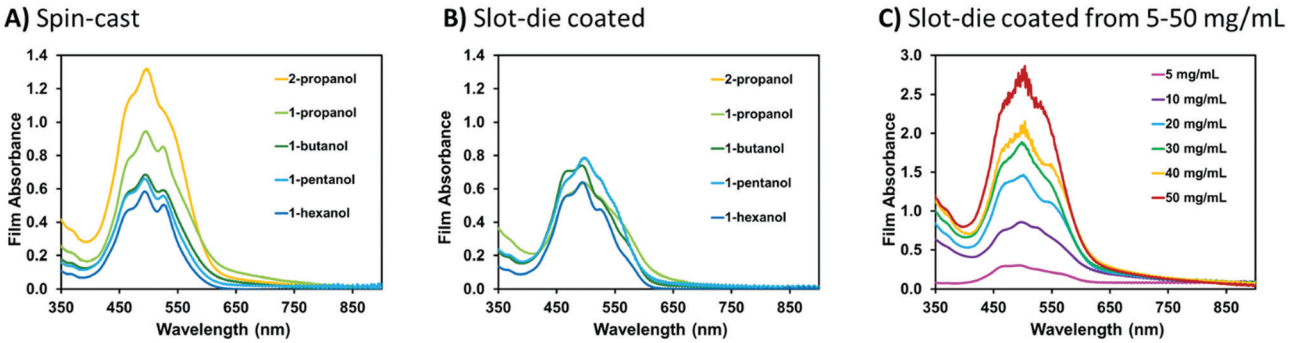

Fig. 5 Optical absorption spectra of (A) PDIN-H films spin-coated from different alcohols at 10 mg mL^{-1}, (B) PDIN-H films slot-die coated from different alcohols at 10 mg mL^{-1}, and (C) PDIN-H films slot-die coated from 1-propranol at varying concentrations onto PET. In all cases 1 molar equivalent NaOH was added to each pre-deposition solution.

subsequent layer. To test the films solvent resistance, we exposed the films to 2-propanol, water, and *o*-xylene. Films were inspected visually, examined using optical and atomic force microscopy, and UV-visible spectra were collected to asses film quality (Fig. 6 and 7). In all cases, no significant dissolution, swelling, cracking, or dewetting of the film was observed. Only with *o*-xylene did we observe any difference as seen in the slight change in the shape of the UV-visible optical absorption spectra. These results demonstrate that PDIN-H can be processed from greener solvents into solvent resistant films. These results were obtained whether the solvent treatment was applied *via* slot-die coating (Fig. 6 and 7) or soaking the films in neat solvent for 10 seconds (Fig. 7 and Fig. S3, ESI†).

The solvent resistance of PDIN-H films likely results from hydrogen bonding between the NH and C=O functional groups of adjacent molecules yielding strong intermolecular coupling. To assess this hypothesis, single crystals of PDIN-H were grown from dioxane/methanol solution (Fig. 8). The crystal structure of PDIN-H shows a distorted perylene core owing to the N-annulation bending the polycyclic aromatic structure.[22] Adjacent molecules of PDIN-H form nanoribbons tightly bound by hydrogen bonds with a NH···O=C distance of 1.96 Å and an angle of 171°. These parameters characterize the hydrogen bonds as moderate with a bond strength of ~4–15 kcal mol^{-1}.[73] DFT analysis of the strength of the hydrogen bond at the M06/6-31G(d,p) level of theory using the supramolecular approach estimates the binding energy of the hydrogen-bonded dimer to be −10.1 kcal mol^{-1}. In the π-stacking direction, PDIN-H forms slightly offset π-stacks with a π–π distance of 3.44 Å (based on the shortest distance between ring centroids). In addition to being offset, the π-stacked molecules are twisted by 37° and tilted by 6.7°, relative to adjacent molecules in the stack, to avoid imide chain interactions. Combined, the tight π-stacks as well as the moderate strength hydrogen bonding explain the solvent resistance of PDIN-H. Further, the tight π-stacking indicates that PDIN-H could function as an electron transport material.

To probe the semiconducting behavior of the PDIN-H films, proof-of-concept organic photovoltaic (OPV) devices were fabricated. PDIN-H was used as an electron transport interlayer (ETL) in inverted type OPV devices to both modify and replace the

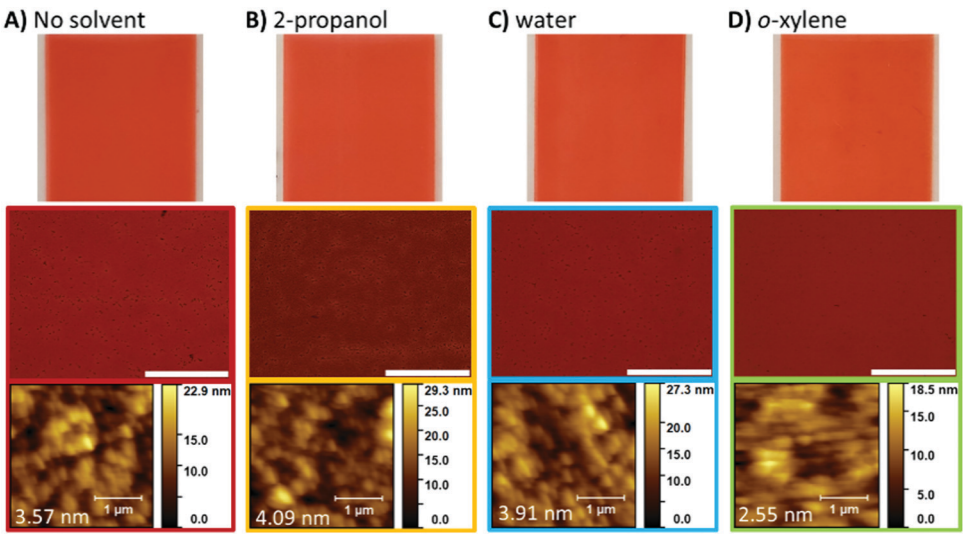

Fig. 6 Photographs of 1.5 cm × 1.5 cm (top), optical microscopy images (10× magnification with white scale bar corresponding to 500 μm) (middle), and atomic force microscopy height images along with the corresponding root mean square roughness RMS (bottom) for PDIN-H films on PET (A) as-cast with no solvent coated on top and with (B) 2-propanol, (C) water, or (D) *o*-xylene slot-die coated on top and left to dry. PDIN-H films were formed *via* slot-die coating 10 mg mL^{-1} PDIN-H solutions in 1-propanol with 1 molar equivalent of NaOH added.

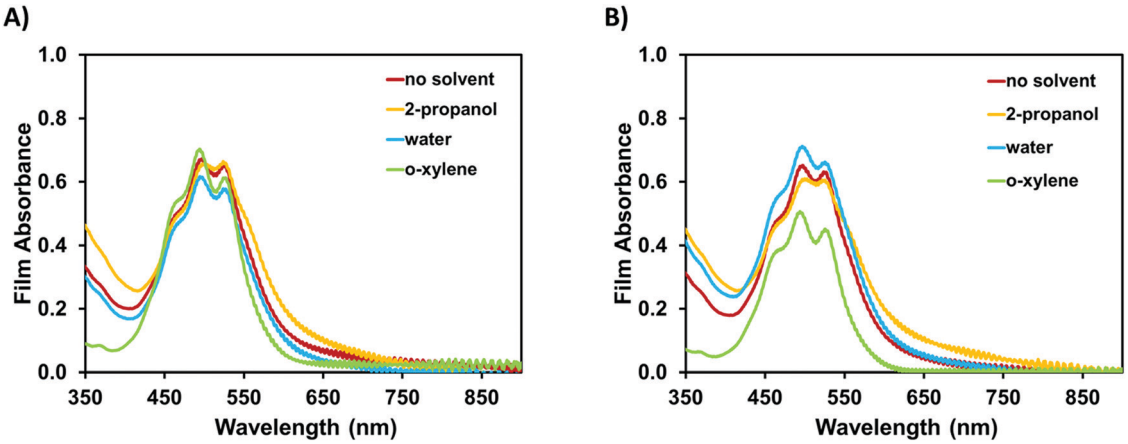

Fig. 7 Optical absorption spectra of PDIN-H films as-cast with no solvent coated on top and with (A) 2-propanol, water, or *o*-xylene slot-die coated on top and left to dry or (B) dipped in 2-propanol, water, or *o*-xylene for 10 s then removed and left to dry.

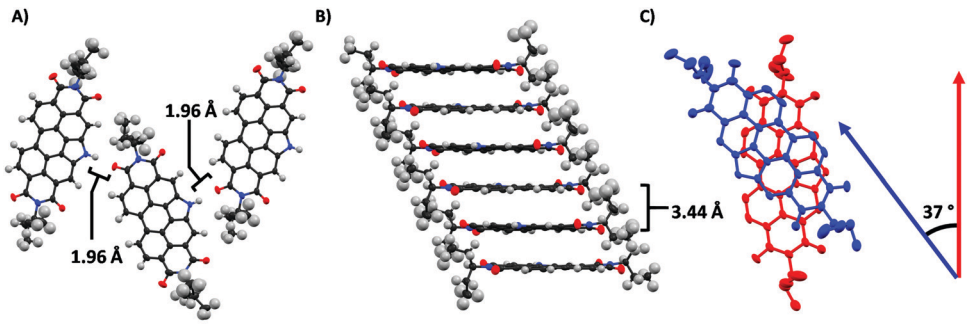

Fig. 8 Structural of PDIN-H highlighting: (A) hydrogen bonding between the NH and C=O functional groups, (B) π–π stacking motif, and (C) the offset and dihedral angle between two π-stacked molecules. In (A) and (B) C, H, N, and O atoms are shown as grey, white, blue, and red, respectively. In (C), H atoms have been omitted for clarity and one molecule of PDIN-H is represented in blue and another in red.

standard ZnO ETL. A device architecture of glass/ITO/ETL/P3HT:$PC_{60}BM$/MoO_x/Al was utilized where ETL = ZnO, ZnO/PDIN-H, or PDIN-H. In all cases the PDIN-H film was formed by spin-coating a 5 mg mL^{-1} solution of PDIN-H in 1-propanol with 1 molar equivalent of NaOH added. The P3HT:$PC_{60}BM$ active layer was selected as it is common to nearly all OPV research laboratories. The device architecture, external quantum efficiency (EQE) spectra, and current density–voltage plots are displayed in Fig. 9 (metrics in Table S2, ESI†). Control devices using a ZnO ETL gave a power conversion efficiency (PCE) of 2.8%, consistent with literature. Use of a ZnO/PDIN-H ETL gave similar PCE of 2.7%. The similar PCE is not unexpected as PDI based materials have been widely used to engineer the ZnO interface.[12,74,75] PDIN-H ETLs performed well, giving similar performance with OPV devices exhibiting a PCE of 2.3%. The slight drop owing to a slightly smaller fill factor (FF) (53% *versus* 60% in the control devices).

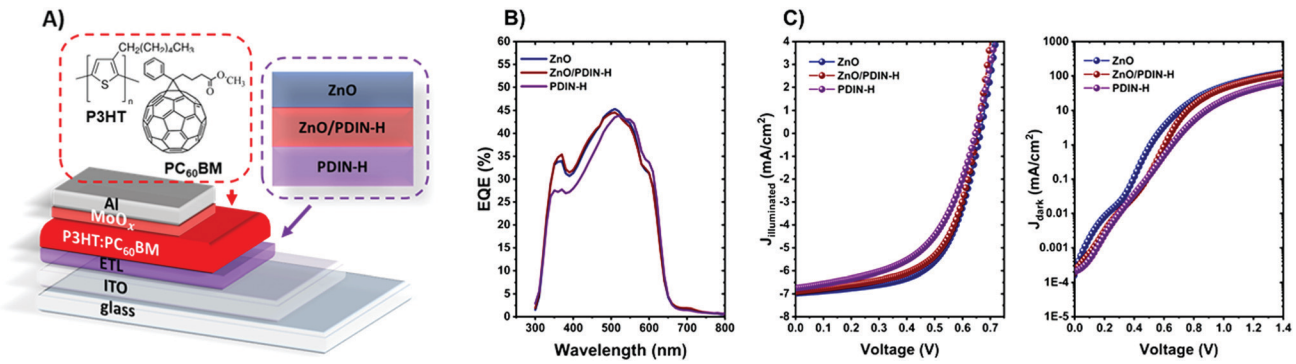

Fig. 9 (A) OPV device architecture. (B) EQE spectra. (C) Current density–voltage characteristics under 1-sun illumination (left) and in the dark (right). PDIN-H layer processed from PDIN-H solutions in 1-propanol with 1 molar equivalent of NaOH added.

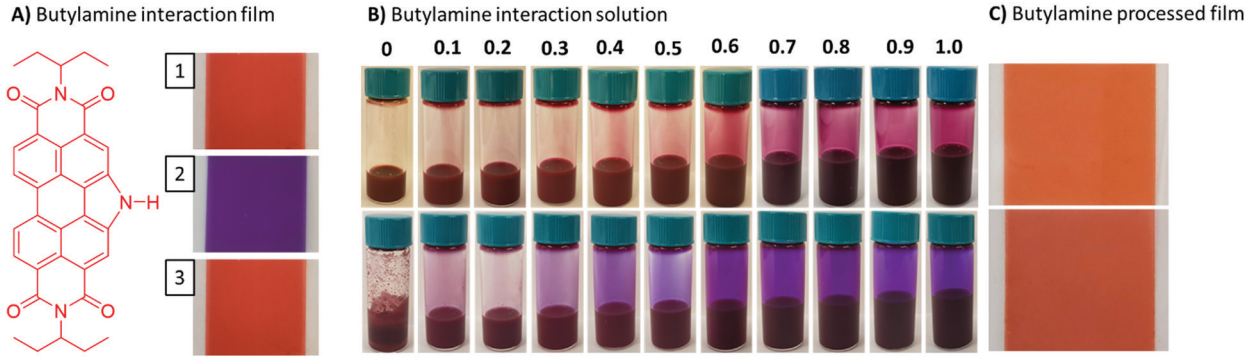

Fig. 10 (A) Chemical structure of PDIN-H and corresponding slot-die coated films (1) as-cast, (2) during exposure to butylamine vapor, and (3) after removal of butylamine vapor. PDIN-H films processed from 10 mg mL^{-1} 1-propanol solutions with 1 molar equivalent NaOH added. (B) Top: PDIN-H in 1-propanol (10 mg mL^{-1}) with added volume equivalents of butylamine. Bottom: PDIN-H in water (10 mg mL^{-1}) with added volume equivalents of butylamine. (C) Photographs of PDIN-H films prepared *via* slot-die coating from: top: 1-propanol/butylamine (1 : 1 v/v) solutions of PDIN-H (5 mg mL^{-1}). Bottom: Water/butylamine (1 : 1 v/v) solutions of PDIN-H (5 mg mL^{-1}).

A lower dark current at voltages >0.6 V in case of the PDIN-H ETL in comparison to the ZnO and ZNO/PDIN-H ETLs suggests that the smaller FF might be due to a higher series resistance at the ITO/PDIN-H interface. Regardless, these proof-of-concept devices demonstrate the utility of the alcohol solvent processed PDIN-H organic films to function as electron transport materials and provides a new material for all-organic PV device fabrication.

To test the viability of water-based processing of the PDIN-H films we tested primary amines as an additive. The rationale is that (1) they are soluble in alcohols and water, and (2) could interact with PDIN-H by polarizing the NH bond and thereby aid solubilizing the material in alcohol or water based solvent systems.[60] To test this hypothesis, we first slot-die coated films of PDIN-H from 1-propanol/NaOH solution then exposed them to butylamine vapor. Indeed, upon exposure in a closed environment, the red PDIN-H film immediately changed color to purple. Simply removing the purple film from the amine vapor and letting sit in air for a few seconds re-established the red color (Fig. 10A). Here the excess butylamine deprotonates the PDIN-H to give the purple PDIN$^-$ anion. When the atmosphere saturated with butylamine is removed, the PDIN$^-$ anion is protonated regenerating the red color, characteristic of PDIN-H, while the butylamine evaporates. No changes in the film were detected by visual inspection and UV-visible spectroscopy (Fig. S5, ESI†).

Next, slurries of PDIN-H in 1-propanol and water were prepared and volume equivalents of butylamine added. For both slurries there was a progressive color change and dissolution of the PDIN-H with increasing volume equivalents of butylamine added. At one volume equivalent complete solvation was observed. (Fig. 10B). The solutions were readily processed into uniform thin-films *via* slot-die coating (Fig. 10C) or spin-coating (Fig. S6, ESI†). The films turned to the characteristic red color of PDIN-H immediately upon film drying. Analysis of the thin films *via* UV-visible spectroscopy showed the signature profile for the PDIN-H, although the water/butylamine processed films were slightly hazy as a result of light scattering (Fig. S6B, ESI†). Regardless, the PDIN-H can be readily processed into uniform thin-films using alcohol or water-based solutions with a volatile amine additive, thus eliminating the need for the use of caustic hydroxide salts. These films showed no significant signs of dissolution, swelling, or cracking upon coating polar and non-polar solvents on top (Fig. S6, ESI†).

Conclusions

In summary, the formation of large area, solvent resistant perylene diimide films has been demonstrated using alcohol and water-based formulations and the roll-to-roll compatible slot-die coating method. The N-annulated perylene diimide, PDIN-H, is a dye with a low solubility in most common solvents that has an intrinsically acidic pyrrolic NH functional group. Upon deprotonation with hydroxide or amine bases the molecule can be fully solubilized in alcohols or water. The purple solutions could be slot-die coated into uniform organic films which spontaneously protonate to give the diagnostic red color of the parent PDIN-H molecule. The films were resistant to both polar and non-polar solvents, a result of the PDIN-H molecule forming tight π–π stacks with significant NH$\cdots$O=C hydrogen bonding in the solid state. This process is reminiscent of acid dyeing of textiles. Proof-of-concept inverted type OPV devices using the alcohol processed films as a replacement for zinc oxide layer showed similar power conversion efficiencies demonstrating the utility of PDIN-H to function as an electron transport layer. This work provides a new design principle for the green solvent processing of organic charge transporting materials that will allow for multi-layered electronic systems to be printed at large scale.

Experimental

Crystal data for PDIN-H, $C_{34}H_{29}N_3O_4$ (M = 543.60 g mol^{-1}): monoclinic, space group $P2_1/c$ (no. 14), a = 18.2166(7) Å, b = 18.5973(10) Å, c = 7.8095(2) Å, β = 97.881(2)°, V = 2620.71(19) Å^3, Z = 4, T = 173 K, μ(CuKα) = 0.734 mm^{-1}, D_{calc} = 1.378 g cm^{-3},

22 039 reflections measured ($4.898^\circ \leq 2\theta \leq 130.452^\circ$), 4467 unique ($R_{int}$ = 0.0349, R_{sigma} = 0.0216) which were used in all calculations. The final R_1 was 0.0581 ($I > 2\sigma(I)$) and wR_2 was 0.1639 (all data).

Conflicts of interest

Work subject to US patent application: Welch, G. C.; Harding, C. R. (Electronically Active, Solvent Resistant Organic Films Processed from Alcohol or Aqueous Media). US Application 63/019,012. May 12, 2020. There are no other potential conflicts of interest.

Acknowledgements

GCW acknowledges CFI JELF (34102), CRC, WED, and the University of Calgary. This work was supported by the NSERC Green Electronics Network (GreEN) (NETGP 508526-17), the NSERC Discovery grants program (RGPIN 2019-04392 and 2014-04940), and the NSERC Strategic grants program (STPGP-521458-2018). AL and MAE acknowledge NSERC for postdoctoral fellowships. JC acknowledges NSERC for a graduate scholarship. This research was undertaken thanks in part to funding from the Canada First Research Excellence Fund (CFREF). KRR and CR acknowledge the National Science Foundation (Cooperative Agreement 1849213) and the Office of Naval Research Young Investigator Program (N00014-18-1-2448) for their support of this project at the University of Kentucky. Supercomputing resources on the Lipscomb High Performance Computing Cluster were provided by the University of Kentucky Information Technology Department and the Center for Computational Sciences (CCS). Martin Kiener (FOR Technologies) is thanked for help and support with the slot-die coating equipment and experiments.

References

1 M. Gsänger, D. Bialas, L. Huang, M. Stolte and F. Würthner, Organic Semiconductors Based on Dyes and Color Pigments, *Adv. Mater.*, 2016, **28**(19), 3615–3645, DOI: 10.1002/adma.201505440.

2 M. Greene, Perylene Pigments, *High Performance Pigments*, John Wiley & Sons, Ltd, 2003, DOI: 10.1002/3527600493.ch16.

3 S. V. Dayneko, M. Pahlevani and G. C. Welch, Indoor Photovoltaics: Photoactive Material Selection, Greener Ink Formulations, and Slot-Die Coated Active Layers, *ACS Appl. Mater. Interfaces*, 2019, **11**(49), 46017–46025, DOI: 10.1021/acsami.9b19549.

4 Y. Zhou, B. Xue, C. Wu, S. Chen, H. Liu, T. Jiu, Z. Li and Y. Zhao, Sulfur-Substituted Perylene Diimides: Efficient Tuning of LUMO Levels and Visible-Light Absorption via Sulfur Redox, *Chem. Commun.*, 2019, **55**(90), 13570–13573, DOI: 10.1039/C9CC07040K.

5 L. Rocard, A. Goujon and P. Hudhomme, Nitro-Perylene-diimide: An Emerging Building Block for the Synthesis of Functional Organic Materials, *Molecules*, 2020, **25**(6), 1402, DOI: 10.3390/molecules25061402.

6 V. Percec, M. Peterca, T. Tadjiev, X. Zeng, G. Ungar, P. Leowanawat, E. Aqad, M. R. Imam, B. M. Rosen, U. Akbey, R. Graf, S. Sekharan, D. Sebastiani, H. W. Spiess, P. A. Heiney and S. D. Hudson, Self-Assembly of Dendronized Perylene Bisimides into Complex Helical Columns, *J. Am. Chem. Soc.*, 2011, **133**(31), 12197–12219, DOI: 10.1021/ja204366b.

7 P.-O. Schwartz, L. Biniek, E. Zaborova, B. Heinrich, M. Brinkmann, N. Leclerc and S. Méry, Perylenediimide-Based Donor–Acceptor Dyads and Triads: Impact of Molecular Architecture on Self-Assembling Properties, *J. Am. Chem. Soc.*, 2014, **136**(16), 5981–5992, DOI: 10.1021/ja4129108.

8 J. Zhang, F. Bai, Y. Li, H. Hu, B. Liu, X. Zou, H. Yu, J. Huang, D. Pan, H. Ade and H. Yan, Intramolecular π-Stacked Perylene-Diimide Acceptors for Non-Fullerene Organic Solar Cells, *J. Mater. Chem. A*, 2019, **7**(14), 8136–8143, DOI: 10.1039/C9TA00343F.

9 A. Nowak-Król, K. Shoyama, M. Stolte and F. Würthner, Naphthalene and Perylene Diimides – Better Alternatives to Fullerenes for Organic Electronics?, *Chem. Commun.*, 2018, **54**(98), 13763–13772, DOI: 10.1039/C8CC07640E.

10 E. Kozma, W. Mróz, F. Villafiorita-Monteleone, F. Galeotti, A. Andicsová-Eckstein, M. Catellani and C. Botta, Perylene Diimide Derivatives as Red and Deep Red-Emitters for Fully Solution Processable OLEDs, *RSC Adv.*, 2016, **6**(66), 61175–61179, DOI: 10.1039/C6RA10467C.

11 R. T. Weitz, K. Amsharov, U. Zschieschang, E. B. Villas, D. K. Goswami, M. Burghard, H. Dosch, M. Jansen, K. Kern and H. Klauk, Organic N-Channel Transistors Based on Core-Cyanated Perylene Carboxylic Diimide Derivatives, *J. Am. Chem. Soc.*, 2008, **130**(14), 4637–4645, DOI: 10.1021/ja074675e.

12 F. Würthner, C. R. Saha-Möller, B. Fimmel, S. Ogi, P. Leowanawat and D. Schmidt, Perylene Bisimide Dye Assemblies as Archetype Functional Supramolecular Materials, *Chem. Rev.*, 2016, **116**(3), 962–1052, DOI: 10.1021/acs.chemrev.5b00188.

13 S. Chen, P. Slattum, C. Wang and L. Zang, Self-Assembly of Perylene Imide Molecules into 1D Nanostructures: Methods, Morphologies, and Applications, *Chem. Rev.*, 2015, **115**(21), 11967–11998, DOI: 10.1021/acs.chemrev.5b00312.

14 G. Li, D. Li, X. Liu, H. Xu, J. Zhang, S. Wang, Z. Liu and B. Tang, Novel Dithiano-Thieno Fused Perylene Diimides: Synthesis, Characterization and Application in Organic Thin-Film Transistors (OTFTs), *Chem. Commun.*, 2019, **55**(65), 9661–9664, DOI: 10.1039/C9CC04133H.

15 Z. Luo, T. Liu, W. Cheng, K. Wu, D. Xie, L. Huo, Y. Sun and C. Yang, A Three-Dimensional Thiophene-Annulated Perylene Bisimide as a Fullerene-Free Acceptor for a High Performance Polymer Solar Cell with the Highest PCE of 8.28% and a VOC over 1.0 V, *J. Mater. Chem. C*, 2018, **6**(5), 1136–1142, DOI: 10.1039/C7TC05261H.

16 D. Meng, D. Sun, C. Zhong, T. Liu, B. Fan, L. Huo, Y. Li, W. Jiang, H. Choi, T. Kim, J. Y. Kim, Y. Sun, Z. Wang and A. J. Heeger, High-Performance Solution-Processed Non-Fullerene Organic Solar Cells Based on Selenophene-Containing Perylene

Bisimide Acceptor, *J. Am. Chem. Soc.*, 2016, **138**(1), 375–380, DOI: 10.1021/jacs.5b11149.

17 Y. Yin, J. Song, F. Guo, Y. Sun, L. Zhao and Y. Zhang, Asymmetrical vs Symmetrical Selenophene-Annulated Fused Perylenediimide Acceptors for Efficient Non-Fullerene Polymer Solar Cells, *ACS Appl. Energy Mater.*, 2018, **1**(11), 6577–6585, DOI: 10.1021/acsaem.8b01484.

18 F. You, X. Zhou, H. Huang, Y. Liu, S. Liu, J. Shao, B. Zhao, T. Qin and W. Huang, N-Annulated Perylene Diimide Derivatives as Non-Fullerene Acceptors for Solution-Processed Solar Cells with an Open-Circuit Voltage of up to 1.14 V, *New J. Chem.*, 2018, **42**(18), 15079–15087, DOI: 10.1039/C8NJ02566E.

19 H. Langhals and S. Kirner, Novel Fluorescent Dyes by the Extension of the Core of Perylenetetracarboxylic Bisimides, *Eur. J. Org. Chem.*, 2000, (2), 365–380, DOI: 10.1002/(SICI)1099-0690(200001)2000:2<365::AID-EJOC365>3.0.CO;2-R.

20 R. K. Gupta, A. Dey, A. Singh, P. K. Iyer and A. A. Sudhakar, Heteroatom Bay-Annulated Perylene Bisimides: New Materials for Organic Field Effect Transistors, *ACS Appl. Electron. Mater.*, 2019, **1**(8), 1378–1386, DOI: 10.1021/acsaelm.9b00004.

21 R. K. Gupta, D. S. Shankar Rao, S. K. Prasad and A. S. Achalkumar, Columnar Self-Assembly of Electron-Deficient Dendronized Bay-Annulated Perylene Bisimides, *Chem. – Eur. J.*, 2018, **24**(14), 3566–3575, DOI: 10.1002/chem.201705290.

22 A. D. Hendsbee, J.-P. Sun, W. K. Law, H. Yan, I. G. Hill, D. M. Spasyuk and G. C. Welch, Synthesis, Self-Assembly, and Solar Cell Performance of N-Annulated Perylene Diimide Non-Fullerene Acceptors, *Chem. Mater.*, 2016, **28**(19), 7098–7109, DOI: 10.1021/acs.chemmater.6b03292.

23 S. M. McAfee, S. V. Dayneko, P. Josse, P. Blanchard, C. Cabanetos and G. C. Welch, Simply Complex: The Efficient Synthesis of an Intricate Molecular Acceptor for High-Performance Air-Processed and Air-Tested Fullerene-Free Organic Solar Cells, *Chem. Mater.*, 2017, **29**(3), 1309–1314, DOI: 10.1021/acs.chemmater.6b04862.

24 S. V. Dayneko, A. D. Hendsbee and G. C. Welch, Fullerene-Free Polymer Solar Cells Processed from Non-Halogenated Solvents in Air with PCE of 4.8%, *Chem. Commun.*, 2017, **53**(6), 1164–1167, DOI: 10.1039/C6CC08939A.

25 A.-J. Payne, S. Li, S. V. Dayneko, C. Risko and G. C. Welch, An Unsymmetrical Non-Fullerene Acceptor: Synthesis via Direct Heteroarylation, Self-Assembly, and Utility as a Low Energy Absorber in Organic Photovoltaic Cells, *Chem. Commun.*, 2017, **53**(73), 10168–10171, DOI: 10.1039/c7cc05836e.

26 S. M. McAfee, A.-J. Payne, S. V. Dayneko, G. P. Kini, C. E. Song, J.-C. Lee and G. C. Welch, A Non-Fullerene Acceptor with a Diagnostic Morphological Handle for Streamlined Screening of Donor Materials in Organic Solar Cells, *J. Mater. Chem. A*, 2017, **5**(32), 16907–16913, DOI: 10.1039/C7TA05282K.

27 S. M. McAfee, S. V. Dayneko, A. D. Hendsbee, P. Josse, P. Blanchard, C. Cabanetos and G. C. Welch, Applying Direct Heteroarylation Synthesis to Evaluate Organic Dyes as the Core Component in PDI-Based Molecular Materials for Fullerene-Free Organic Solar Cells, *J. Mater. Chem. A*, 2017, **5**(23), 11623–11633, DOI: 10.1039/C7TA00318H.

28 S. V. Dayneko, A. D. Hendsbee and G. C. Welch, Combining Facile Synthetic Methods with Greener Processing for Efficient Polymer-Perylene Diimide Based Organic Solar Cells, *Small Methods*, 2018, **2**(6), 1800081, DOI: 10.1002/smtd.201800081.

29 S. M. McAfee, A.-J. Payne, A. D. Hendsbee, S. Xu, Y. Zou and G. C. Welch, Toward a Universally Compatible Non-Fullerene Acceptor: Multi-Gram Synthesis, Solvent Vapor Annealing Optimization, and BDT-Based Polymer Screening, *Sol. RRL*, 2018, **2**(9), 1800143, DOI: 10.1002/solr.201800143.

30 S. M. McAfee and G. C. Welch, Development of Organic Dye-Based Molecular Materials for Use in Fullerene-Free Organic Solar Cells, *Chem. Rec.*, 2019, **19**(6), 989–1007, DOI: 10.1002/tcr.201800114.

31 F. Tintori, A. Laventure and G. C. Welch, Perylene Diimide Based Organic Photovoltaics with Slot-Die Coated Active Layers from Halogen-Free Solvents in Air at Room Temperature, *ACS Appl. Mater. Interfaces*, 2019, **11**(42), 39010–39017, DOI: 10.1021/acsami.9b14251.

32 S. V. Dayneko, M. Pahlevani and G. C. Welch, Indoor Photovoltaics: Photoactive Material Selection, Greener Ink Formulations, and Slot-Die Coated Active Layers, *ACS Appl. Mater. Interfaces*, 2019, **11**(49), 46017–46025, DOI: 10.1021/acsami.9b19549.

33 M. Irimia-Vladu, E. D. Głowacki, G. Voss, S. Bauer and N. S. Sariciftci, Green and Biodegradable Electronics, *Mater. Today*, 2012, **15**(7), 340–346, DOI: 10.1016/S1369-7021(12)70139-6.

34 M. Irimia-Vladu, ''Green'' Electronics: Biodegradable and Biocompatible Materials and Devices for Sustainable Future, *Chem. Soc. Rev.*, 2014, **43**(2), 588–610, DOI: 10.1039/C3CS60235D.

35 D. J. Burke and D. J. Lipomi, Green Chemistry for Organic Solar Cells, *Energy Environ. Sci.*, 2013, **6**(7), 2053–2066, DOI: 10.1039/C3EE41096J.

36 R. Po and J. Roncali, Beyond Efficiency: Scalability of Molecular Donor Materials for Organic Photovoltaics, *J. Mater. Chem. C*, 2016, **4**(17), 3677–3685, DOI: 10.1039/C5TC03740A.

37 S. Zhang, L. Ye, H. Zhang and J. Hou, Green-Solvent-Processable Organic Solar Cells, *Mater. Today*, 2016, **19**(9), 533–543, DOI: 10.1016/j.mattod.2016.02.019.

38 L. Ye, Y. Xiong, Z. Chen, Q. Zhang, Z. Fei, R. Henry, M. Heeney, B. T. O'Connor, W. You and H. Ade, Sequential Deposition of Organic Films with Eco-Compatible Solvents Improves Performance and Enables Over 12%-Efficiency Nonfullerene Solar Cells, *Adv. Mater.*, 2019, **31**(17), 1808153, DOI: 10.1002/adma.201808153.

39 D. Prat, A. Wells, J. Hayler, H. Sneddon, C. R. McElroy, S. Abou-Shehada and P. J. Dunn, CHEM21 Selection Guide of Classical- and Less Classical-Solvents, *Green Chem.*, 2015, **18**(1), 288–296, DOI: 10.1039/C5GC01008J.

40 Y. Diao, L. Shaw, Z. Bao and S. C. B. Mannsfeld, Morphology Control Strategies for Solution-Processed Organic Semiconductor Thin Films, *Energy Environ. Sci.*, 2014, **7**(7), 2145–2159, DOI: 10.1039/C4EE00688G.

41 Z. Ma, B. Zhao, Y. Gong, J. Deng and Z. Tan, Green-Solvent-Processable Strategies for Achieving Large-Scale Manufacture of Organic Photovoltaics, *J. Mater. Chem. A*, 2019, **7**(40), 22826–22847, DOI: 10.1039/C9TA09277C.

42 B. Schmatz, Z. Yuan, A. W. Lang, J. L. Hernandez, E. Reichmanis and J. R. Reynolds, Aqueous Processing for Printed Organic Electronics: Conjugated Polymers with Multistage Cleavable Side Chains, *ACS Cent. Sci.*, 2017, **3**(9), 961–967, DOI: 10.1021/acscentsci.7b00232.

43 B. V. Khau, L. R. Savagian, M. De Keersmaecker, M. A. Gonzalez and E. Reichmanis, Carboxylic Acid Functionalization Yields Solvent-Resistant Organic Electrochemical Transistors, *ACS Mater. Lett.*, 2019, **1**(6), 599–605, DOI: 10.1021/acsmaterialslett.9b00373.

44 Z. Li, L. Ying, P. Zhu, W. Zhong, N. Li, F. Liu, F. Huang and Y. Cao, A Generic Green Solvent Concept Boosting the Power Conversion Efficiency of All-Polymer Solar Cells to 11%, *Energy Environ. Sci.*, 2019, **12**(1), 157–163, DOI: 10.1039/C8EE02863J.

45 C. Zhang and S. Holdcroft, Photocrosslinking of Low Band-Gap Conjugated Polymers Using Alkyl Chloride Sidechains: Toward High-Efficiency, Thermally Stable Polymer Solar Cells, *J. Mater. Res.*, 2018, **33**(13), 1879–1890, DOI: 10.1557/jmr.2018.78.

46 R.-Q. Png, P.-J. Chia, J.-C. Tang, B. Liu, S. Sivaramakrishnan, M. Zhou, S.-H. Khong, H. S. O. Chan, J. H. Burroughes, L.-L. Chua, R. H. Friend and P. K. H. Ho, High-Performance Polymer Semiconducting Heterostructure Devices by Nitrene-Mediated Photocrosslinking of Alkyl Side Chains, *Nat. Mater.*, 2009, **9**(2), 152–158, DOI: 10.1038/nmat2594.

47 J. W. Rumer and I. McCulloch, Organic Photovoltaics: Crosslinking for Optimal Morphology and Stability, *Mater. Today*, 2015, **18**(8), 425–435, DOI: 10.1016/J.MATTOD.2015.04.001.

48 K. Hunger, *Industrial Dyes: Chemistry, Properties, Applications*, Wiley-VCG Verlag GmbH& Co. KgaA, Weinheim, Germany, 1st edn, 2003, DOI: 10.1002/3527602011.ch5.

49 J. Ho, V. E. Zwicker, K. K. Y. Yuen and K. A. Jolliffe, Quantum Chemical Prediction of Equilibrium Acidities of Ureas, Deltamides, Squaramides, and Croconamides, *J. Org. Chem.*, 2017, **82**(19), 10732–10736, DOI: 10.1021/acs.joc.7b02083.

50 G. C. Shields and P. G. Seybold, *Computational Approaches for the Prediction of pKa Values*, CRC Press, Boca Raton, Florida, 1st edn, 2013, DOI: 10.1201/b16128.

51 M. D. Liptak and G. C. Shields, Accurate PKa Calculations for Carboxylic Acids Using Complete Basis Set and Gaussian-n Models Combined with CPCM Continuum Solvation Methods, *J. Am. Chem. Soc.*, 2001, **123**(30), 7314–7319, DOI: 10.1021/ja010534f.

52 D. M. Chipman, Computation of PKa from Dielectric Continuum Theory, *J. Phys. Chem. A*, 2002, **106**(32), 7413–7422, DOI: 10.1021/jp020847c.

53 R. F. Ribeiro, A. V. Marenich, C. J. Cramer and D. G. Truhlar, Use of Solution-Phase Vibrational Frequencies in Continuum Models for the Free Energy of Solvation, *J. Phys. Chem. B*, 2011, **115**(49), 14556–14562, DOI: 10.1021/jp205508z.

54 J. Ho, Are Thermodynamic Cycles Necessary for Continuum Solvent Calculation of PKas and Reduction Potentials?, *Phys. Chem. Chem. Phys.*, 2014, **17**(4), 2859–2868, DOI: 10.1039/C4CP04538F.

55 Y. Zhao and D. G. Truhlar, The M06 Suite of Density Functionals for Main Group Thermochemistry, Thermochemical Kinetics, Noncovalent Interactions, Excited States, and Transition Elements: Two New Functionals and Systematic Testing of Four M06-Class Functionals and 12 Other Functionals, *Theor. Chem. Acc.*, 2008, **120**(1), 215–241, DOI: 10.1007/s00214-007-0310-x.

56 P. C. Hariharan and J. A. Pople, The Influence of Polarization Functions on Molecular Orbital Hydrogenation Energies, *Theor. Chim. Acta*, 1973, **28**(3), 213–222, DOI: 10.1007/BF00533485.

57 G. A. Petersson, A. Bennett, T. G. Tensfeldt, M. A. Al-Laham, W. A. Shirley and J. Mantzaris, A Complete Basis Set Model Chemistry. I. The Total Energies of Closed-shell Atoms and Hydrides of the First-row Elements, *J. Chem. Phys.*, 1988, **89**(4), 2193–2218, DOI: 10.1063/1.455064.

58 G. A. Petersson and M. A. Al-Laham, A Complete Basis Set Model Chemistry. II. Open-shell Systems and the Total Energies of the First-row Atoms, *J. Chem. Phys.*, 1991, **94**(9), 6081–6090, DOI: 10.1063/1.460447.

59 A. V. Marenich, C. J. Cramer and D. G. Truhlar, Universal Solvation Model Based on Solute Electron Density and on a Continuum Model of the Solvent Defined by the Bulk Dielectric Constant and Atomic Surface Tensions, *J. Phys. Chem. B*, 2009, **113**(18), 6378–6396, DOI: 10.1021/jp810292n.

60 M. Vespa, J. R. Cann, S. V. Dayneko, O. A. Melville, A. D. Hendsbee, Y. Zou, B. H. Lessard and G. C. Welch, Synthesis of a Perylene Diimide Dimer with Pyrrolic N–H Bonds and N-Functionalized Derivatives for Organic Field-Effect Transistors and Organic Solar Cells, *Eur. J. Org. Chem.*, 2018, (33), 4592–4599, DOI: 10.1002/ejoc.201801055.

61 X. Wen, A. Nowak-Król, O. Nagler, F. Kraus, N. Zhu, N. Zheng, M. Müller, D. Schmidt, Z. Xie and F. Würthner, Tetrahydroxy-Perylene Bisimide Embedded in a Zinc Oxide Thin Film as an Electron-Transporting Layer for High-Performance Non-Fullerene Organic Solar Cells, *Angew. Chem., Int. Ed.*, 2019, **58**(37), 13051–13055, DOI: 10.1002/anie.201907467.

62 E. He, J. Wang, H. Xu, Z. He, H. Wang, H. Zhao, Y. Zhang, R. Zhang and H. Zhang, Facile Synthesis of Graphene Oxide Sheet-Immobilized Perylene Diimide Radical Anion Salt and Its Optical Response to Different Solvents and PH Values, *J. Mater. Sci.*, 2016, **51**(14), 6583–6589, DOI: 10.1007/s10853-016-9885-8.

63 C. Capello, U. Fischer and K. Hungerbühler, What Is a Green Solvent? A Comprehensive Framework for the Environmental Assessment of Solvents, *Green Chem.*, 2007, **9**(9), 927–934, DOI: 10.1039/B617536H.

64 R. Søndergaard, M. Hösel, D. Angmo, T. T. Larsen-Olsen and F. C. Krebs, Roll-to-Roll Fabrication of Polymer Solar Cells, *Mater. Today*, 2012, **15**(1), 36–49, DOI: 10.1016/S1369-7021(12)70019-6.

65 A. Sandström, H. F. Dam, F. C. Krebs and L. Edman, Ambient Fabrication of Flexible and Large-Area Organic Light-Emitting Devices Using Slot-Die Coating, *Nat. Commun.*, 2012, **3**(1), 1–5, DOI: 10.1038/ncomms2002.

66 J. Alstrup, M. Jørgensen, A. J. Medford and F. C. Krebs, Ultra Fast and Parsimonious Materials Screening for Polymer

Solar Cells Using Differentially Pumped Slot-Die Coating, *ACS Appl. Mater. Interfaces*, 2010, **2**(10), 2819–2827, DOI: 10.1021/am100505e.

67 F. C. Krebs, Polymer Solar Cell Modules Prepared Using Roll-to-Roll Methods: Knife-over-Edge Coating, Slot-Die Coating and Screen Printing, *Sol. Energy Mater. Sol. Cells*, 2009, **93**(4), 465–475, DOI: 10.1016/j.solmat.2008.12.012.

68 M. Hösel, H. F. Dam and F. C. Krebs, Development of Lab-to-Fab Production Equipment Across Several Length Scales for Printed Energy Technologies, Including Solar Cells, *Energy Technol.*, 2015, **3**(4), 293–304, DOI: 10.1002/ente.201402140.

69 A. Namepetra, E. Kitching, A. F. Eftaiha, I. G. Hill and G. C. Welch, Understanding the Morphology of Solution Processed Fullerene-Free Small Molecule Bulk Heterojunction Blends, *Phys. Chem. Chem. Phys.*, 2016, **18**(18), 12476–12485, DOI: 10.1039/C6CP01269H.

70 M. Nazari, E. Cieplechowicz, T. A. Welsh and G. C. Welch, A Direct Comparison of Monomeric vs. Dimeric and Non-Annulated vs. N-Annulated Perylene Diimide Electron Acceptors for Organic Photovoltaics, *New J. Chem.*, 2019, **43**(13), 5187–5195, DOI: 10.1039/C8NJ06491A.

71 F. C. Spano, The Spectral Signatures of Frenkel Polarons in H- and J-Aggregates, *Acc. Chem. Res.*, 2010, **43**(3), 429–439, DOI: 10.1021/ar900233v.

72 F. Bencheikh, D. Duché, C. M. Ruiz, J.-J. Simon and L. Escoubas, Study of Optical Properties and Molecular Aggregation of Conjugated Low Band Gap Copolymers: PTB7 and PTB7-Th, *J. Phys. Chem. C*, 2015, **119**(43), 24643–24648, DOI: 10.1021/acs.jpcc.5b07803.

73 T. W. Steiner, The Hydrogen Bond in the Solid State, *Angew. Chem., Int. Ed.*, 2002, **41**(1), 48–76, DOI: 10.1002/1521-3773(20020104)41:1<48::AID-ANIE48>3.0.CO;2-U.

74 Z. Xie and F. Würthner, Hybrid Photoconductive Cathode Interlayer Materials Composed of Perylene Bisimide Photosensitizers and Zinc Oxide for High Performance Polymer Solar Cells, *Adv. Energy Mater.*, 2017, **7**(16), 1602573, DOI: 10.1002/aenm.201602573.

75 M. Abd-Ellah, J. Cann, S. V. Dayneko, A. Laventure, E. Cieplechowicz and G. C. Welch, Interfacial ZnO Modification Using a Carboxylic Acid Functionalized N-Annulated Perylene Diimide for Inverted Type Organic Photovoltaics, *ACS Appl. Electron. Mater.*, 2019, **1**(8), 1590–1596, DOI: 10.1021/acsaelm.9b00328.